

## DETERMINATION OF BAND STRUCTURE AND COMPTON PROFILES FOR ALUMINUM-ARSENIDE USING DENSITY FUNCTIONAL THEORY<sup>†</sup>

Sameen F. Mohammed<sup>a</sup>,  Salah M.A. Ridha<sup>b</sup>,  Abdulhadi Mirdan Ghaleb<sup>b,\*</sup>,  Zahraa Talib Ghaleb<sup>c</sup>,  
 Yamina Benkrima<sup>d</sup>, Mahran Abdulrhman Abdullah<sup>e</sup>

<sup>a</sup>Department of Mechanical Techniques, Technical institute Kirkuk, Northern Technical University, Iraq

<sup>b</sup>Department of Physics, College of Science, University of Kirkuk, Iraq

<sup>c</sup>Department Chemistry, College of Science, University of Kirkuk, Kirkuk, Iraq

<sup>d</sup>Department of Exact Sciences, ENS Ouargla, Algeria

<sup>e</sup>Ministry of Education, Kirkuk Education Directorate, Iraq

\*Corresponding author e-mail: [abdlhadig4@gmail.com](mailto:abdlhadig4@gmail.com)

Received March 21, 2023; revised April 14, 2023; accepted April 15, 2023

First-principles computations of the electronic structure of AIAs have been carried out using the density functional theory (DFT) within Local Density Approximation-LDA and Generalized Gradient Approximation - GGA. We utilized the CASTEP's plane wave basis set implementation for the total energy computation (originally from Cambridge Serial Total Energy Package). We have used to examine structure parameter in structure of AIAs The electronic structure calculation using the two approximations show that the LDA and the GGA methods underestimated the band gap while the band gap predicted by the GGA is closer to the experimental result. according to the electronic structure calculation utilizing the two approximations. The GGA calculation shows a direct band-gap semiconductor of 2.5 eV. The energy band diagram is used to calculate the total and partial densities of AIAs states. Multiple configurations of the ionic model were calculated for  $Al^{1+x}As^{-x}$  ( $0.0 \leq x \leq 1$ ) also performed utilizing free-atom profiles. According to the ionic model, 0.75 electrons would be transferred from the valence 5p state of aluminium to the 3p state of Arsenide.

**Keywords:** *generalized gradient approximation; localized density approximation; Density functional theory; energy band gap; density of states; Ionic model; Compton profiles*

**PACS:**02.70.-c, 71.15.Ap, 71.15.Mb, 17.20.-b, 71.15.Dx , 73.20.At

### 1. INTRODUCTION

Groups III–V have been the focus of a great deal of research during the past few decades. LEDs, lasers, photo detectors, integrated circuits, modulators, and filters are only some of the electronic and optoelectronic devices that benefit from the AIAs compound [1]. These compounds often crystallize into the zincblende (ZB) form under standard circumstances [2]. AIAs's band structure has only been fully calculated using a SCOPW model by Stukel and Euwema [3]. There is a several theoretical calculations of the electrical structures of AIAs over the past two decades [4–6]. But to our knowledge, only fitting methods like the tight-binding model [7,8,9] exist. Almost all theoretical analyses of the AIAs band structure have produced band gaps that differ to variable degrees from the actual values [4–6,10–13]. Density-functional-theory (DFT) [14,15] was used to conduct first-principles calculations [16], and the open-source software package Quantum ESPRESSO was used to approximate the exchange-correlation functional using the local density approximation. Existing theories and experiments are linked to the outcomes achieved. They have come to a satisfactory accord. The electrical, optical, and structural characteristics of AIAs are the subject of a variety of theoretical investigations [3,17–25]. However, because to its high hygroscopicity [26–29], very few experimental experiments are conducted on bulk AIAs. Stukel and Euwema [3] presented energy band calculations for cubic AIAs using a first-principles plane-wave approach self-consistent orthogonalized. Using the pseudo potential approach in the local density approximation, Cohen and Froyen [17] investigated the structural properties of various III-V semiconductor compounds and the static, including Aluminum-Arsenide (LDA). Many researchers [19–21] have published AIAs's electrical characteristics, total energy, effective mass, lattice constants, etc. Using the empirical pseudo potential technique, Joshi and Sharma [22] reported a few years ago on the theoretical directional Compton profiles of AIP and Aluminum-Arsenide. (EPM). This paper is structured as follows: in Section 2, presented the paper's theoretical framework and computational details. Section 3 contains the discussion and results in the final section have been provided a conclusion.

### 2. METHODOLOGY DETAILS

#### 2.1. Computation Method

The ion-electron interactions in the electronic structure computations have been performed using the non-local ultra soft pseudo potential developed by Vanderbilt [30]. The computations employed the LDA with the Ceperley Alder PerdewZunger [31] and the GGA with the Perdew-Burke Ernzerh of Solid [32] exchange correlation potentials. Al  $3s^2 3p^1$  and As  $4s^2 4p^3$  are studied by pseudo-atom computations. Total energy converges to  $0.5E-05$  eV/atom, which is self-consistent. Our estimates' convergence is verified through in-depth exploration of the interplay between the k-point

<sup>†</sup> **Cite as:** S.F. Mohammed, S.M.A. Ridha, A.M. Ghaleb, Z.T. Ghaleb, Y. Benkrima, and M.A. Abdullah, East Eur. J. Phys. 2, 132 (2023), <https://doi.org/10.26565/2312-4334-2023-2-12>

© S.F. Mohammed, S.M.A. Ridha, A.M. Ghaleb, Z.T. Ghaleb, Y. Benkrima, M.A. Abdullah, 2023

and the cut-off energy set mesh on the Monk horst-Pack grid. For the computational expense, we use a Monk horst-Pack mesh with  $16 \times 16 \times 16$  k-points for the Brillouin zone sample and a plane wave basis set with an energy cutoff of 800 eV. In addition, Vanderbilt's [30] non-local ultra soft pseudo potential is used. Kramer's-Kronig transform accuracy and the energy range that can be accounted for are both sensitive to the number of conduction bands that are included in the calculation. The electrical structure is investigated here by employing the Cambridge Serial Total Energy Package (CASTEP) [33,34], which takes into account not only the occupied bands but also the 16 unoccupied ones.

## 2.2. Ionic model

The free atom profiles-FA of Aluminum and Arsenide, the data were taken from a table Biggs [35], were used to produce the theoretical Compton profiles of Aluminum-Arsenide for various ionic configurations. We were able to identify the valence profiles of a wide variety of  $\text{Al}^{+x}\text{As}^{-x}$  (x ranges from 0 to 1) combinations by transferring an electron from Al's 3p or 3s shell into As's 4p shell. The valence profiles were combined to the core contributions to generate the entire profiles [36], which were then normalized to  $(19.966e^-)$  in the range of 0 to 7 a.u. in order to give a direct comparison with other studied in the same experimental data [37].

## 3. RESULTS AND DISCUSSION

### 3.1. Electronic properties

Herein, density functional theory (using LDA and GGA) was used to examine the electrical characteristics of the binary compound AlAs in the zinc mix structure. Researchers have found that AlAs exhibits a direct band gap (G-G). You can see the outcomes in Fig. 1 (a and b).

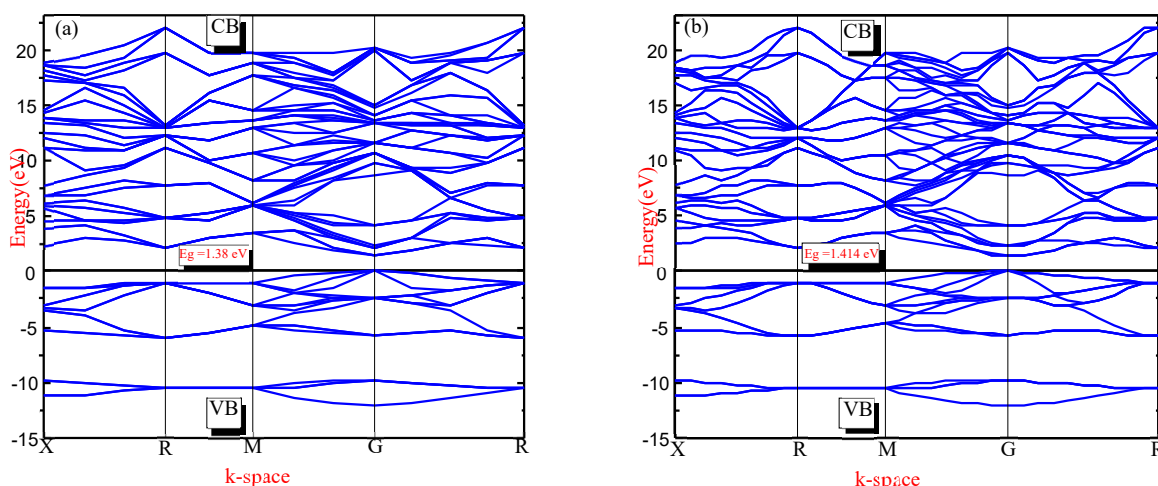


**Figure 1.** Band gap structure of AlAs applying (a) LDA and (b) GGA approximation

The band gap values generated by GGA are more in line with the known experimental results than the LDA values. The LDA is known to consistently understate the energy gap [38]. The GGA technique can provide a more stable band structure because it is based on potential optimization. Band gap values computed using the GGA approach fare far better in comparison to experiment than those produced using the LDA method. Our recent calculations indicate that the GGA approximation performs a decent job of characterizing the band features, and that the GGA results may be compared to those produced using more expensive approaches, such as GW and hybrid functional for band gaps. It can be used to simulate the electronic characteristics of semiconductors. It has a direct band gap of 1.38 eV (LDA) and 1.415 eV (GGA), with the valence and conduction band minimums both located at the G point. The measured findings are roughly in agreement with our calculated band gap size [39]. Using the data shown in Fig. 1, we can see that the Fermi energy of aluminum arsenide (AlAs) is 0.699 eV (LDA) and 0.689 eV (GGA), and that the G-point symmetry point is where the valence band-VB is at its maximum and the conduction band-CB is at its minimum. As the valence band maximum and conduction band minimum are positioned on distinct symmetry points, AlAs is a direct band gap semiconductor with an energy gap value of 1.38 eV (LDA) and 1.414 eV. The Al 3p-like and 3s-like electrons and the As 4p-like electrons are responsible for the 3 bands found below the Fermi level. Because of the presence of Al 3p-like states and as 4p-like ones, the conduction bands-CB above the Fermi level are empty. The theoretical values for Aluminum-Arsenide [40] correspond with the calculated energy gaps. The higher ionic nature of AlAs causes it to exhibit a wider optical band gap and a higher rate of charge transfer. These similarities in structure also explain why it exhibits metallic and covalent characteristics. AlAs is commonly used in applications that need higher temperature operation due to its broad band gap, which pointing to the ability of Aluminum-Arsenide for higher photon energy in reflectivity measurements. As a result of their direct band gap and large band gap, they are a prospective option for use in semiconductor technology. Because of this, it is also used as an active material in the production of LEDs and other optoelectronic devices. Applications in the technology of

higher power and higher frequency electronic devices in the short wave length region have also gained traction. Light-emitting diodes, blue and ultraviolet lasers, photo detectors, optical pumping devices, and hetero structures all rely on AlAs as a fundamental material [41,42].

### 3.2. Density of State

According to the Density of State Diagram for AlAs, the 4p states of As and 3p states of Al are responsible for the small peaks in Fig. 2(a and b) above its Fermi energy. The p-like and s-like electrons of as are what give rise to the longer peaks near the Fermi energy. The third zone is composed of the top (2) valence bands, which are mostly p-like. The anion state, which is comparable to that of the alkali halides, displays both the density of states and the band structure [43,44].

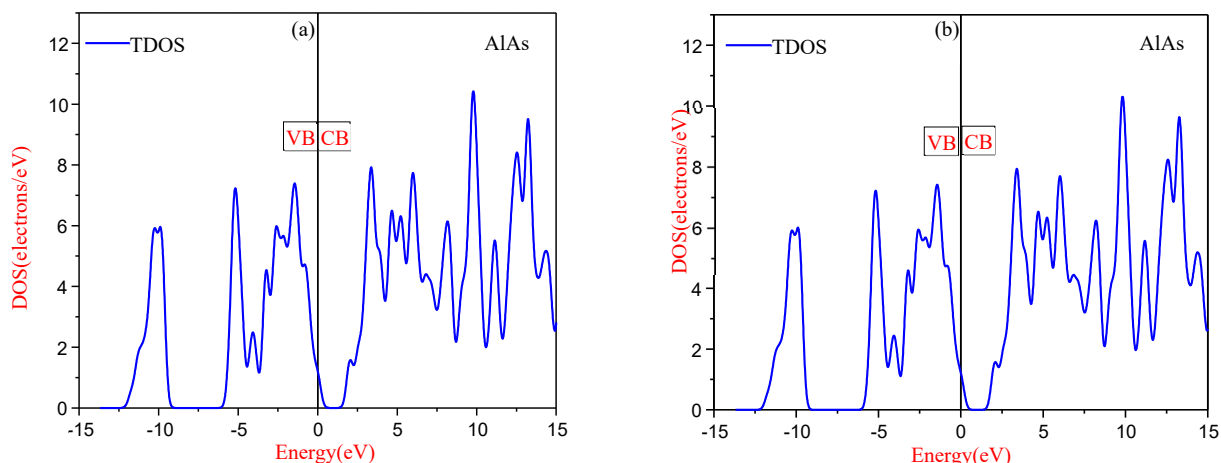


Figure 2. The total density of states of compounds binary AlAs using the LDA and GGA approaches

### 3.3. Charge Transfer

Particularly, Figure (3) illustrates. The current study uses theoretical approaches as opposed to earlier research, which relied on experimental valence Compton profiles of the elemental solids [37].

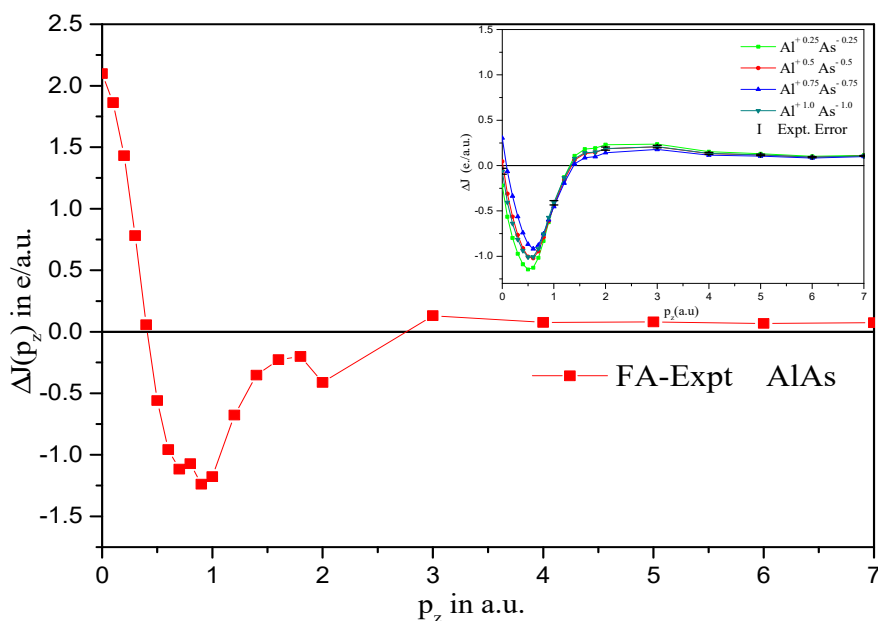


Figure 3. Comparison of the theoretical and experimental Compton profiles of AlAs. The measuring of the differences between various ionic configurations [37].

We have also included free atom valence profiles in the current charge transfer analysis. The 4s 4p states of As and the 3s 3p states of Al are included in these profiles. In the inset, we see the matching difference profiles (convoluted

ionic - experiment) shown. Importantly, it is necessary to convolute the ionic profiles with the resolution function of the instrument and to normalize them to the free atom area, which is equal to 19.967 electrons. For 0 to 7 a.u. before a comparison of ionic values with experimental data can be made [37]. From the inset, it is clear that the effect of changing charges on As and Al is not noticeable until the charge reaches 1.5 a.u. All ionic configurations behave identically and overlap at distances greater than 1.5 a.u. We have calculated  $\chi^2$  as follows, which allows us to test the global concordance of all ionic configurations with the experiment:

$$\chi^2 = \sum_{p_z=0}^7 \left| \frac{\Delta J(p_z)}{\sigma(p_z)} \right|^2 \quad (1)$$

where  $\sigma(p_z)$  represents a random error in the experiment [37]. According to  $\chi^2$  tests, the best agreement among the ionic structures is found in the  $Al^{3.0}As^{-3.0}$  state.

According to the basic ionic model, the charge in this molecule must flow from Aluminum to Arsenide. The same explanations are also given in the ref [36]. However, this process requires three electrons to be transferred from  $Al3s^23p^1$  state to  $As4s^24p^3$  state, indicating that AlAs bonds primarily through ionic interactions. There is a clear limitation of the ionic model in the low momentum area, where the discrepancies between the convoluted ionic and experimental profiles are quite large. It is worth noting that the ionic model's predicted charge transfer is greater than the value derived by a different technique [37].

#### 4. CONCLUSIONS

The present research summarizes the results of a density functional theory (DFT) analysis of electronic AlAs Compound in the LDA and GGA approximations. Following is a brief synopsis of the key findings: The direct gap at G is the only exception; otherwise, our calculated band gaps agree quite well with the experimental findings. The intrinsic property of LDA pseudo potentials means that the estimated band gap values are smaller than the experimental values. The reason for this is the reduced complexity of the exchange correlation functional. The estimated electronic band structure reveals that AlAs is a Semiconductors with a direct band gap of 1.38 eV (LDA) and 1.414 eV (GGA), respectively. When compared to other theoretical calculations obtained, this shows a significant improvement. Semiconductors have conducting properties, as indicated by the fact that the DOS energy level within them reveals a particularly high situation of electron occupation and that the DOS seen near the Fermi level for semiconductors is zero. For the spherically averaged electron momentum density (EMD), there is good agreement between the measured and estimated values. Calculations using the ionic model for a variety of  $(Al^{+x})(As^{-x})$  ( $x$  varies from 0 to 1), combinations result in a 0.75 electron transfer from the  $3s^2 3p^1$  Aluminum valence state to the  $4s^2 4p^3$  Arsenide valence state.

#### ORCID IDs

Salah M.A. Ridha, <https://orcid.org/0000-0003-0569-3849>; Abdulhadi Mirdan Ghaleb, <https://orcid.org/0000-0002-2202-8827>; Zahraa Talib Ghaleb, <https://orcid.org/0000-0003-0569-3849>, Yamina Benkrima, <https://orcid.org/0000-0001-8005-4065>

#### REFERENCES

- [1] R. Ahmed, S.J. Hashemifar, H. Akbarzadeh, and M. Ahmed, "Ab initio study of structural and electronic properties of III-arsenide binary compounds," *Computational materials science*, **39**(3), 580-586 (2007). <https://doi.org/10.1016/j.commatsci.2006.08.014>
- [2] A. Mujica, A. Rubio, A. Munoz, and R.J. Needs, "High-pressure phases of group-IV, III-V, and II-VI compounds," *Reviews of modern physics*, **75**(3), 863(2003). <https://doi.org/10.1103/RevModPhys.75.863>
- [3] D.J. Stukel, and R.N. Euwema, "Energy-band structure of aluminum arsenide," *Physical Review*, **188**(3), 1193 (1969). <https://doi.org/10.1103/PhysRev.188.1193>
- [4] B.I. Min, S. Massidda, and A.J. Freeman, "Structural and electronic properties of bulk GaAs, bulk AlAs, and the  $(GaAs)_1(AlAs)_1$  superlattice," *Physical Review B*, **38**(3), 1970 (1988). <https://doi.org/10.1103/PhysRevB.38.1970>
- [5] M.Z. Huang, and W.Y. Ching, "Calculation of optical excitations in cubic semiconductors. I. Electronic structure and linear response," *Physical Review B*, **47**(15), 9449 (1993). <https://doi.org/10.1103/PhysRevB.47.9449>
- [6] S. Lebègue, B. Arnaud, M. Alouani, and P.E. Bloechl, "Implementation of an all-electron GW approximation based on the projector augmented wave method without plasmon pole approximation: Application to Si, SiC, AlAs, InAs, NaH, and KH," *Physical Review B*, **67**(15), 155208 (2003). <https://doi.org/10.1103/PhysRevB.67.155208>
- [7] T.B. Boykin, "Generalized eigenproblem method for surface and interface states: The complex bands of GaAs and AlAs," *Physical Review B*, **54**(11), 8107 (1996). <https://doi.org/10.1103/PhysRevB.54.8107>
- [8] J.P. Loehr, and D.N. Talwar, "Exact parameter relations and effective masses within sp<sup>3</sup> zinc-blende tight-binding models," *Physical Review B*, **55**(7), 4353 (1997). <https://doi.org/10.1103/PhysRevB.55.4353>
- [9] A.B. Chen, and A. Sher, "Electronic structure of III-V semiconductors and alloys using simple orbitals," *Physical Review B*, **22**(8), 3886 (1980). <https://doi.org/10.1103/PhysRevB.22.3886>
- [10] R.W. Godby, M. Schlüter, and L.J. Sham, "Quasiparticle energies in GaAs and AlAs," *Physical Review B*, **35**(8), 4170 (1987). <https://doi.org/10.1103/PhysRevB.35.4170>
- [11] P. Boguslawski, and I. Gorczyca, "Influence of chemistry on the energy band structure: AlAs versus GaAs," *Acta Physica Polonica, A*, **80**(3), 433-436 (1991). <http://dx.doi.org/10.12693/APhysPolA.80.433>
- [12] B.K. Agrawal, and S. Agrawal, "Ab initio calculation of the electronic, structural, and dynamical properties of AlAs and CdTe," *Physical Review B*, **45**(15), 8321 (1992). <https://doi.org/10.1103/PhysRevB.45.8321>
- [13] Q. Guo, C.K. Ong, H.C. Poon, and Y.P. Feng, "Calculation of electron effective masses in AlAs," *Physica Status Solidi (b)*, **197**(1), 111-117 (1996). <https://doi.org/10.1002/pssb.2221970117>

- [14] P. Hohenberg, and W. Kohn, "Inhomogeneous electron gas," *Physical review*, **136**(3B), B864 (1964). <https://doi.org/10.1103/PhysRev.136.B864>
- [15] W. Kohn, and L.J. Sham, "Self-consistent equations including exchange and correlation effects," *Physical review*, **140**(4A), A1133 (1965). <https://doi.org/10.1103/PhysRev.140.A1133>
- [16] P. Giannozzi, S. Baroni, N. Bonini, M. Calandra, R. Car, C. Cavazzoni, D. Ceresoli, et al., "QUANTUM ESPRESSO: a modular and open-source software project for quantum simulations of materials," *Journal of physics: Condensed matter*, **21**(39), 395502 (2009). <https://doi.org/10.1088/0953-8984/21/39/395502>
- [17] S. Froyen, and M.L. Cohen, "Structural properties of III-V zinc-blende semiconductors under pressure," *Physical Review B*, **28**(6), 3258 (1983). <https://doi.org/10.1103/PhysRevB.28.3258>
- [18] A. Mujica, R.J. Needs, and A. Munoz, "First-principles pseudopotential study of the phase stability of the III-V semiconductors GaAs and AlAs," *Physical Review B*, **52**(12), 8881 (1995). <https://doi.org/10.1103/PhysRevB.52.8881>
- [19] M. Städele, M. Moukara, J.A. Majewski, P. Vogl, and A. Görling, "Exact exchange Kohn-Sham formalism applied to semiconductors," *Physical Review B*, **59**(15), 10031 (1999). <https://doi.org/10.1103/PhysRevB.59.10031>
- [20] A.R. Jivani, H.J. Trivedi, P.N. Gajjar, and A.R. Jani, "Total energy, equation of state and bulk modulus of AIP, AlAs and AlSb semiconductors," *Pramana*, **64**(1), 153-158 (2005). <https://doi.org/10.1007/BF02704540>
- [21] H. Jin, G.L. Zhao, and D. Bagayoko, "Density functional band gaps of AlAs," *Physical Review B*, **73**(24), 245214 (2006). <https://doi.org/10.1103/PhysRevB.73.245214>
- [22] K.B. Joshi, and B.K. Sharma, "Compton profile study of AlAs and AIP by empirical pseudopotential method," *Proceedings-national academy of sciences India, Section A*, **76**(1), 79 (2006). [http://nasi.nic.in/76\\_a\\_I\\_14.htm](http://nasi.nic.in/76_a_I_14.htm)
- [23] J. Cai, and N. Chen, "Theoretical study of pressure-induced phase transition in AlAs: From zinc-blende to NiAs structure," *Physical Review B*, **75**(17), 174116 (2007). <https://doi.org/10.1103/PhysRevB.75.174116>
- [24] N. Fraj, I. Saïdi, S.B. Radhia, and K. Boujdaria, "Band structures of AlAs, GaP, and SiGe alloys: A 30 k×p model," *Journal of Applied Physics*, **102**(5), 053703 (2007). <https://doi.org/10.1063/1.2773532>
- [25] H. Arabshahi, M.R. Khalvati, and M.R. Rokn-Abadi, "Temperature and doping dependencies of electron mobility in InAs, AlAs and AlGaAs at high electric field application," *Brazilian Journal of Physics*, **38**, 293-296 (2008). <https://doi.org/10.1590/S0103-97332008000300001>
- [26] B. Monemar, "Optical Dispersion and Ionicity of AIP and AlAs," *Physica Scripta*, **3**(3-4), 193 (1971). <https://doi.org/10.1088/0031-8949/3/3-4/015>
- [27] B. Monemar, "Fundamental energy gaps of AlAs and AIP from photoluminescence excitation spectra," *Physical Review B*, **8**(12), 5711-5718 (1973). <https://doi.org/10.1103/PhysRevB.8.5711>
- [28] A. Onton, and R.J. Chicotka, "Free-exciton-impurity interaction in AlAs," *Physical Review B*, **10**(2), 591 (1974). <https://doi.org/10.1103/PhysRevB.10.591>
- [29] R.G. Greene, H. Luo, T. Li, and A.L. Ruoff, "Phase transformation of AlAs to NiAs structure at high pressure," *Physical review letters*, **72**(13), 2045 (1994). <https://doi.org/10.1103/PhysRevLett.72.2045>
- [30] D. Vanderbilt, "Soft self-consistent pseudopotentials in a generalized eigenvalue formalism," *Physical review B*, **41**(11), 7892 (1990). <https://doi.org/10.1103/PhysRevB.41.7892>
- [31] J.P. Perdew, A. Ruzsinszky, G.I. Csonka, O.A. Vydrov, G.E. Scuseria, L.A. Constantin, X. Zhou, and K. Burke, "Restoring the density-gradient expansion for exchange in solids and surfaces," *Physical review letters*, **100**(13), 136406 (2008). <https://doi.org/10.1103/PhysRevLett.100.136406>
- [32] S.H. Vosko, L. Wilk, and M. Nusair, "Accurate spin-dependent electron liquid correlation energies for local spin density calculations: a critical analysis," *Canadian Journal of physics*, **58**(8), 1200-1211 (1980). <https://doi.org/10.1139/p80-159>
- [33] V. Milman, B. Winkler, J.A. White, C.J. Pickard, M.C. Payne, E.V. Akhmatkaya, and R.H. Nobes, "Electronic structure, properties, and phase stability of inorganic crystals: A pseudopotential plane-wave study," *International Journal of Quantum Chemistry*, **77**(5), 895-910 (2000). [https://doi.org/10.1002/\(SICI\)1097-461X\(2000\)77:5%3C895::AID-QUA10%3E3.0.CO;2-C](https://doi.org/10.1002/(SICI)1097-461X(2000)77:5%3C895::AID-QUA10%3E3.0.CO;2-C)
- [34] M.C. Payne, M.P. Teter, D.C. Allan, T.A. Arias, and A.J. Joannopoulos, "Iterative minimization techniques for ab initio total-energy calculations: molecular dynamics and conjugate gradients," *Reviews of modern physics*, **64**(4), 1045 (1992). <https://doi.org/10.1103/RevModPhys.64.1045>
- [35] F. Biggs, L.B. Mendelsohn, and J.B. Mann, "Hartree-Fock Compton profiles for the elements," *Atomic data and nuclear data tables*, **16**(3), 201-309 (1975). [https://doi.org/10.1016/0092-640X\(75\)90030-3](https://doi.org/10.1016/0092-640X(75)90030-3)
- [36] S.F. Mohammed, A.M. Ghaleb, and E.S. Ali, "Electron Momentum Density of Nan particles ZrO2: A Compton Profile Study," *International Journal of Nanoscience*, **20**(02), 2150018 (2021). <https://doi.org/10.1142/S0219581X21500186>
- [37] G. Sharma, K.B. Joshi, M.C. Mishra, R.K. Kothari, Y.C. Sharma, V. Vyas, and B.K. Sharma, "Electronic structure of AlAs: a Compton profile study," *Journal of alloys and compounds*, **485**(1-2), 682-686 (2009). <http://dx.doi.org/10.1016%2Fj.jallcom.2009.06.043>
- [38] A.M. Ghaleb, A.T. Shihatha, and Z.T. Ghaleb, "Investigation of the physical properties and Mulliken charge distribution of the cube perovskite BiGaO<sub>3</sub> is calculated by GGA-PBE," *Digest Journal of Nanomaterials and Biostructures (DJNB)*, **17**(4), (2022). <https://doi.org/10.15251/DJNB.2022.174.1181>
- [39] M.P. Thompson, G.W. Auner, T.S. Zheleva, K.A. Jones, S.J. Simko, and J.N. Hilfiker, "Deposition factors and band gap of zinc-blende AlN," *Journal of Applied Physics*, **89**(6), 3331-3336 (2001). <https://doi.org/10.1063/1.1346999>
- [40] K. Boubendir, H. Meradji, S. Ghemid, and F.E.H. Hassan, "Theoretical prediction of the structural, electronic, and thermal properties of Al<sub>1-x</sub>B<sub>x</sub>As ternary alloys," *Materials science in semiconductor processing*, **16**(6), 2063-2069 (2013). <https://doi.org/10.1016/j.mssp.2013.07.022>
- [41] D. Kirin, and I. Lukačević, "Stability of high-pressure phases in II-VI semiconductors by a density functional lattice dynamics approach," *Physical Review B*, **75**(17), 172103 (2007). <https://doi.org/10.1103/PhysRevB.75.172103>
- [42] A.M. Ghaleb, and A.Q. Ahmed, "Structural, electronic, and optical properties of sphalerite ZnS compounds calculated using density functional theory (DFT)," *Chalcogenide Letters*, **19**(5), 309-318 (2022). <https://doi.org/10.15251/CL.2022.195.309>

- [43] C.N. Louis, and K. Iyakutti, "Electronic phase transition and superconductivity of vanadium under high pressure," *Physical Review B*, **67**(9), 094509 (2003). <https://doi.org/10.1103/PhysRevB.67.094509>
- [44] A.T. Shihatha, A.M. Ghaleb, and R.A. Munfi, "Theoretical study of electronic structure and optical properties for ZnO thin film," *AIP Conference Proceedings*, **2398**(1), 020023 (2022). <https://doi.org/10.1063/5.0094037>

### ВИЗНАЧЕННЯ ЗОННОЇ СТРУКТУРИ ТА КОМПТОН ПРОФІЛІВ ДЛЯ АРСЕНІДУ АЛЮМІНІЮ З ВИКОРИСТАННЯМ ФУНКЦІОНАЛУ ГУСТИНИ

Самін Ф. Мохаммед<sup>a</sup>, Салах М.А. Рідха<sup>b</sup>, Абдулхаді Мірдан Галеб<sup>b</sup>, Захра Таліб Галеб<sup>c</sup>,  
Яміна Бенкріма<sup>d</sup>, Махран Абдулрхман Абдулла<sup>e</sup>

<sup>a</sup>Кафедра механічних технологій, Технічний інститут Кіркук, Північний технічний університет, Ірак

<sup>b</sup>Факультет фізики, Науковий коледж, Університет Кіркука, Ірак

<sup>c</sup>Кафедра хімії Наукового коледжу Кіркукського університету, Кіркук, Ірак

<sup>d</sup>Департамент точних наук, ENS Уаргла, Алжир

<sup>e</sup>Міністерство освіти, Директорат освіти Кіркука, Ірак

Основні розрахунки електричних характеристик AlAs були проведені з використанням теорії функціоналу щільності (DFT) і локальної щільності (LDA), методів (DFT) і узагальненої градієнтної апроксимації (GGA). Ми використали реалізацію базового набору плоских хвиль CASTEP для обчислення загальної енергії (спочатку з Cambridge Serial Total Energy Package). Раніше ми дивилися на структурний параметр структури AlAs. Ширина забороненої зони була переоцінена за допомогою узагальненої градієнтної апроксимації та методів LDA, хоча ширина забороненої зони, передбачена GGA, більше відповідає експериментальним висновкам, згідно з розрахунком електронної структури з використанням двох наближень. За допомогою GGA розрахунку виявлено напівпровідник із шириною забороненої зони 2,5 еВ. Енергетична зонна діаграма була використана для розрахунку повної та часткової густини станів AlAs. Було розраховано кілька конфігурацій іонної моделі.  $Al^{+x}As^{-x}$  ( $0.0 \leq x \leq 1$ ) також виконуються з використанням профілів вільних атомів. Відповідно до іонної моделі, 0,75 електрона буде перенесено з валентного 5p-стану алюмінію в 3p-стан арсеніду.

**Ключові слова:** узагальнена градієнтна апроксимація; апроксимація локалізованої щільності; теорія функціонала густини; енергетична заборонена зона; щільність станів; іонна модель; Комптон-профілі